IOPscience iopscience.iop.org

Home Search Collections Journals About Contact us My IOPscience

# An analytical study of resistive oxygen gas sensors

This article has been downloaded from IOPscience. Please scroll down to see the full text article.

2008 J. Phys.: Condens. Matter 20 145204

(http://iopscience.iop.org/0953-8984/20/14/145204)

View the table of contents for this issue, or go to the journal homepage for more

Download details:
IP Address: 129.252.86.83
The article was downloaded on 29/05/2010 at 11:27

Please note that terms and conditions apply.

J. Phys.: Condens. Matter **20** (2008) 145204 (6pp) doi:10.1088/0953-8984/20/14/145204

# An analytical study of resistive oxygen gas sensors

**M Souri[1], M N Azarmanesh[1], E Abbaspour Sani[2], M Nasseri[1] and Kh Farhadi[3]**

[1] Department of Physics, Faculty of Science, Urmia University, Urmia, Iran
[2] Department of Electrical Engineering, Urmia University, Urmia, Iran
[3] Department of Chemistry, Faculty of Science, Urmia University, Urmia, Iran

E-mail: e.abbaspour@mail.urmia.ac.ir

Received 4 November 2007, in final form 13 February 2008
Published 18 March 2008
Online at stacks.iop.org/JPhysCM/20/145204

**Abstract**

The effects of oxygen gas pressure and operating temperature on the sensing layer of resistive oxygen gas sensors are analytically studied. We include the effects of the temperature, gas pressure, energy gap, Fermi energy, and concentration of the electrons and holes. To achieve more accurate equations for the temperature and gas pressure dependency of the oxide semiconductor sensing layers, Fermi–Dirac distribution is employed instead of the conventionally used Boltzman function. Consequently, we have derived new equations that give the variation of conductivity of the sensing layer as a function of operating temperature and gas pressure more accurately. To examine the exactness of our derived equations, the responses of $CeO_2$ and $SrTi_{0.65}Fe_{0.35}O_{3-\delta}$ based oxygen gas sensors as a function of temperature and gas pressure are calculated using Matlab software. The obtained results are in close agreement with the reported measured results.

(Some figures in this article are in colour only in the electronic version)

## 1. Introduction

The precise measurement of oxygen concentration has gained great importance in a variety of fields, including those of combustion control, food preservation, experimental measurement, biology, medical engineering, industry, and control of large combustion furnaces [1]. Resistive sensors have been investigated intensively in recent years. Due to their simplicity, low cost, small size, IC-process compatibility, measurement circuit simplification, and low power consumption, resistive oxygen gas sensors stand out among the other types of sensors [2].

Oxygen sensors based on $CeO_2$, $TiO_2$, $Ga_2O_3$, $BaTiO_3$ (Nb), $TiO_2$(Nb, Cr), and $SrTiO_3$ are at an advanced stage of development [3–7]. These sensors operate at a high temperature (500–1200 °C) and are used to detect the gases exhausted by car engines or during metallurgical processes. In many materials, such as $SnO_2$, $SnO_2$(Li), $SnO_2$/Pt, ZnO, ZnO(Li), $Cu_2O$, and $Nb_2O_5$, surface effects induce a conductance variation, and hence these materials have been employed in sensors designed for detecting low oxygen pressures (1–1000 mbar) at low and medium temperatures (200–500 °C) [8–10].

The main disadvantage of the oxide semiconductor resistive oxygen sensor is their dependency on temperature [11]. The resistive oxygen gas sensors are sensitive to temperature because, not only does it influence the physical properties of oxide semiconductor sensing layers such as variation of free carrier concentration, the energy gap, and the Fermi energy, but also because it affects the reaction taking place on the semiconductor which determines the most probable species adsorbed and hence, the reaction sites. Since the operating temperature has a considerable effect on the response of resistive oxygen gas sensors, a detailed study of this is of great importance.

## 2. Theoretical study

The general expression for the dependency of the electrical conductivity, $\sigma$ of the resistive sensing layer and the operating temperature is given by [12]:

$$\sigma \propto e^{E_A/kT}. \quad (1)$$

 © 2008 IOP Publishing Ltd Printed in the UK

The above relation does not consider the temperature dependency of some parameters such as activation energy $E_A$ and mobility, which are also a function of temperature. We will investigate the effect of the most effective parameters and introduce new equations for sensor response. The n-type and p-type sensing oxide layer semiconductors will be studied separately.

### *2.1. Resistive oxygen gas sensors based on n-type semiconductors*

The general expression for the electrical conductivity of n-type semiconductors is given by [12]:

$$\sigma_e = q\mu_e n_e \tag{2}$$

where $q$ is the electron charge, $\mu_e$ is the electron mobility, and $n_e$ is the electron concentration. It should be noted that both $\mu_e$ and $n_e$ are temperature-dependent and one should take account of both of these terms when the sensing layers are studied.

The mobility is temperature-dependent and can be determined by experiment or calculation. However, it will be of the form [13]:

$$\mu_e = \mu_0 T^{-m} \tag{3}$$

where $\mu_0$ is a constant, $T$ is the temperature, and $m$ is the power exponent. For crystalline semiconductors with low level of defect concentration (<1%), $m = 1.5$ at high temperature, but $m$ may be considerably larger (e.g. $m = 4.5$) in disordered semiconductors due to charge localization and dislocations. So the dependency of mobility on temperature cannot always be ignored.

We will mainly concentrate on evaluating the dependency of $n_e$ on operating temperature and the detecting gas pressure.

*2.1.1. Evaluating concentration of electrons n as a function of the temperature and oxygen pressure.* The concentration of electrons in the conduction band can be determined by solving the following integral [14]:

$$n = \int_{E_g}^{\infty} D_e(E) f_e(E)\, dE \tag{4}$$

where $(D_e(E))$ is the density of states and $f_e(E)$ is the occupation probability and they are respectively given by:

$$D_e(E) = \frac{1}{2\pi}\left(\frac{2m_e}{\hbar^2}\right)^{1.5}(E - E_g)^{\frac{1}{2}}, \qquad f_e(E) = \frac{1}{e^{\frac{(E-E_f)}{kT}}}. \tag{5}$$

If we assume $E - E_f \gg K_B T$ for the conduction band of a semiconductor, the Fermi–Dirac distribution function reduces to the Boltzman distribution function. Considering this assumption and substituting equations (5) in (4) we obtain the approximated equation for $n$ as:

$$n = 2\left(\frac{m_e kT}{2\pi\hbar^2}\right)^{1.5}\exp\left(\frac{E_f - E}{kT}\right). \tag{6}$$

To calculate the concentration of the electrons '$n$' more accurately, we employed the Fermi–Dirac function in equation (4) instead of the Boltzman function and $n$ was derived by solving the following equation:

$$n = \frac{1}{2\pi}\left(\frac{2m_e}{\hbar^2}\right)^{1.5}\int_{E_g}^{\infty}(E - E_g)^{\frac{1}{2}} \times \frac{1}{e^{\frac{(E-E_f)}{kT}} + 1}\, dE. \tag{7}$$

To solve the above integral, first of all, we have to evaluate the general form of integral: $\int_0^{\infty} \frac{x^s}{Ae^x + 1}\, dx$.

In doing so, the more accurate equation for the concentration of electrons is derived:

$$n = \frac{\sqrt{\pi}}{4\pi^2}\left(\frac{2m_e k}{\hbar^2}\right)^{1.5} T^{1.5}\sum_{n=0}^{\infty}\frac{(-1)^n}{(n+1)^{1.5}} e^{-(n+1)(E_g - E_f)/kT} \tag{8}$$

where, $E_g$ and $E_f$ are the energy gap and Fermi energy, respectively.

The Fermi energy of oxide semiconductors used as oxygen sensing layers is affected by oxygen gas pressure and temperature. We have derived the governing equation and the final result is:

$$E_f = E_{f,0} - \left(\frac{kT}{2(\gamma + 1)}\right) Ln\left(\frac{p_{O_2}}{p_{O_{2,0}}}\right) \tag{9}$$

where $E_{f,0}$ is the Fermi energy at a reference oxygen pressure $P_{O_{2,0}}$ and $\gamma$ equals 1 or 2 depending on the number of ionized oxygen vacancies.

We can practically measure the variable $E_{f,0}$ (e.g. by the Hall effect method) and obtain its value for a reference oxygen pressure.

The temperature dependency of the energy gap for semiconductors is fitted by the following empirical relation [15]:

$$E_g(T) = E_g(0) - \frac{\alpha T^2}{\beta + T} \tag{10}$$

where $E_g(0)$ is the value of the energy gap at 0 K, $\alpha$ and $\beta$ are constants.

Substituting equations (3), (8), (9), and (10) in equation (2), the general and more accurate equation for the electrical conductivity of the oxygen gas sensors is obtained:

$$\sigma_e = \frac{q\mu_0}{4}\left(\frac{2m_e k}{\pi\hbar^2}\right)^{1.5} T^{1.5-m}\left[\sum_{n=0}^{\infty}\frac{(-1)^n}{(n+1)^{1.5}} \times e^{-(n+1)(E_g(0) - E_{f,0}\frac{\alpha T^2}{\beta+T})/kT}\left(\frac{P_{O_2}}{P_{O_{2,0}}}\right)^{\frac{-(n+1)}{2(\gamma+1)}}\right]. \tag{11}$$

As it is clear from equation (11), the conductivity of n-type oxide semiconductor oxygen sensing layers is affected by operating temperature and oxygen gas pressure.

### *2.2. Resistive oxygen gas sensors based on p-type oxide semiconductors*

The same procedure as carried out for the n-type oxide semiconductors is applied to the p-type sensing layers. The obtained results indicate that the electrical conductivity of the

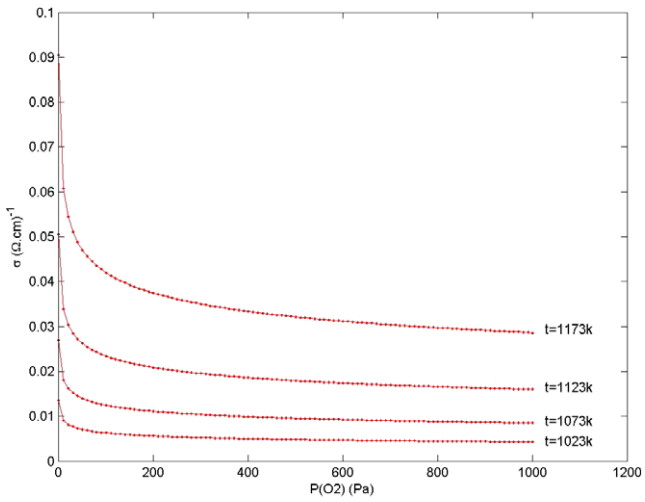


**Figure 1.** The conductivity of the ceria sensor versus oxygen pressure for four different temperatures.

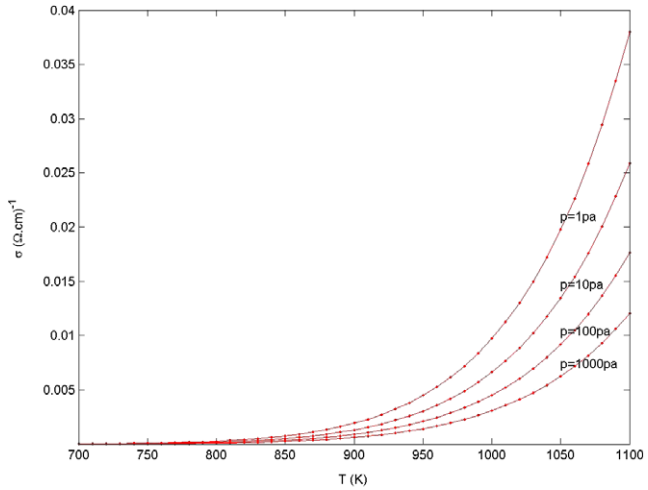


**Figure 2.** The conductivity of the $CeO_2$ sensor versus operating temperature at different pressures.

p-type oxide semiconductors also depends on the operating temperature and oxygen pressure. The derived relationship is:

$$\sigma_h = \frac{q\mu_0}{4}\left(\frac{2m_h k}{\pi\hbar^2}\right)^{1.5} T^{1.5-m} \times \left[\sum_{n=0}^{\infty}\frac{(-1)^n}{(n+1)^{1.5}} e^{-(n+1)E_{f,0}/kT}\left(\frac{Po_2}{Po_{2,0}}\right)^{\frac{(n+1)}{2(\gamma+1)}}\right]. \quad (12)$$

## 3. Analytical results

The derived equations (11) and (12) for the conductivity of the sensing layers were investigated by substituting the appropriate reported values for the parameters based on the n-type and p-type oxygen sensing layer. The graphs of conductivity versus temperature and pressure were plotted using Matlab software. The results for n-type and p-type layers will be discussed separately.

### *3.1. N-type sensing layers based on $CeO_2$*

Since $CeO_2$ is an n-type oxide semiconductor and its operation temperature is high, it can be a good candidate to investigate equation (11) derived for n-type sensing layers. The substituted values of the parameters required in equation (11) were as the values reported by Kosacki [15]:

$$E_g(0) = 3.4\ \text{eV}, \qquad E_{f,0} = 2.5\ \text{eV},$$
$$P(O_2)_0 = 2\times 10^{-2}\ \text{Pa}, \qquad m = -1.7,$$
$$\alpha = 4.5\times 10^{-4}, \qquad \beta = 514.2 \qquad \text{and} \qquad \gamma = 2.$$

The graphs of conductivity versus oxygen gas pressure and temperature using equation (11) and Matlab software are shown in figures 1 and 2, respectively.

### *3.2. P-type oxygen sensing layers based on $SrTi_{0.65}Fe_{0.35}O_{3-\delta}$*

Recently, $SrTi_{0.65}Fe_{0.35}O_{3-\delta}$, due to its strong sensitivity to oxygen pressure, has received considerable attention for use as a resistive oxygen sensor. On the other hand, since

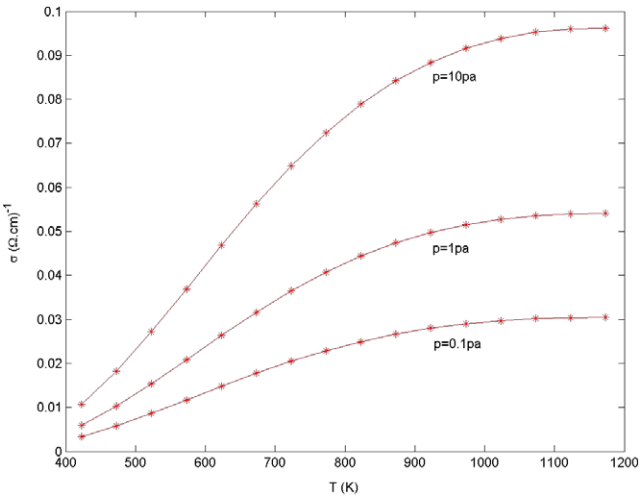


**Figure 3.** Plot of the response of the $SrTi_{0.65}Fe_{0.35}O_{3-\delta}$ sensor as a function of the operating temperature at different pressures.

$SrTi_{0.65}Fe_{0.35}O_{3-\delta}$ is a p-type semiconductor at high oxygen pressure, we can use our equation (12) and plot conductivity as a function of temperature and oxygen gas pressure and investigate its effects. Figure 3 shows the response of the $SrTi_{0.65}Fe_{0.35}O_{3-\delta}$ sensor as a function of temperature at different oxygen pressures using equation (12) and the value of the required parameters as: $E_{f,0} = 0.3$ eV, $P(O_2)_0 = 2\times 10^4$ Pa, $m = 4.5$ and $\gamma = 1$ [16].

It is clear from our calculated results shown in figure 3, that at high temperatures (>900 K) the electrical conductivity is independent of temperature, as is the case with the measured result reported by Litzelman *et al* [16].

In figure 4 the conductivity of $SrTi_{0.65}Fe_{0.35}O_{3-\delta}$ as a function of oxygen pressure at five different temperatures using equation (12) and Matlab software is shown.

As indicated in figure 4, the calculated electrical conductivity increases with increasing oxygen pressure, which is expected according to the reported measurement results [16].

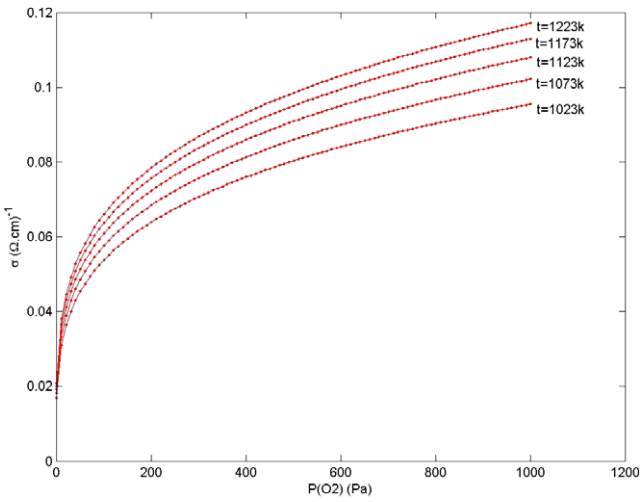


**Figure 4.** Conductivity versus oxygen pressure for $SrTi_{0.65}Fe_{0.35}O_{3-\delta}$ based sensors at five different temperatures.

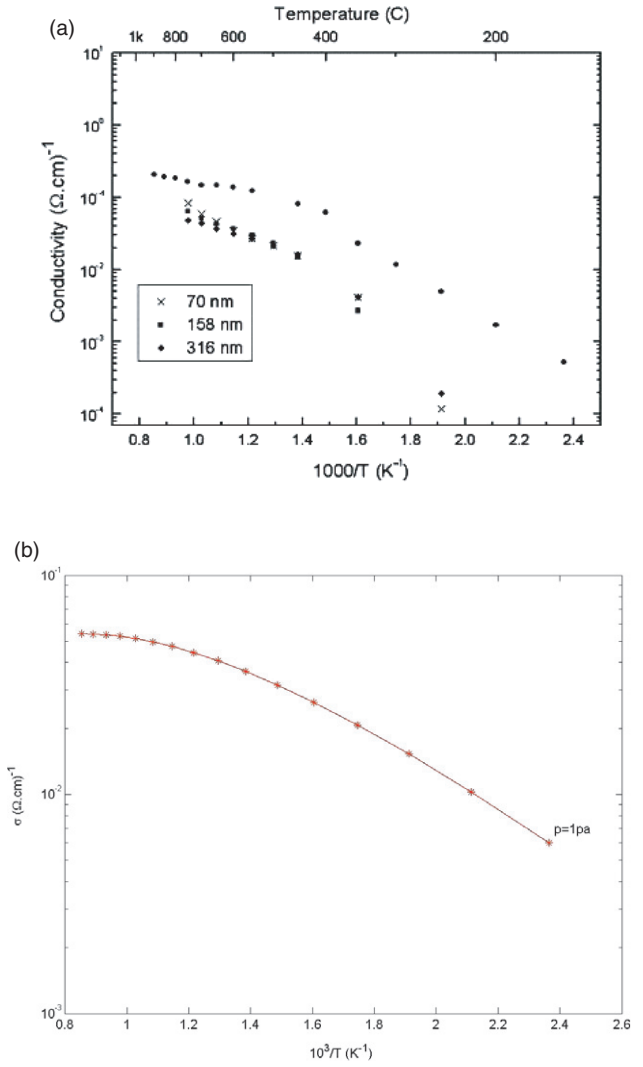


**Figure 5.** Calculated and measured results for $SrTi_{0.65}Fe_{0.35}O_{3-\delta}$ based sensors. (a) The measurement results by Scott Litzelman [16] and (b) the calculated results.

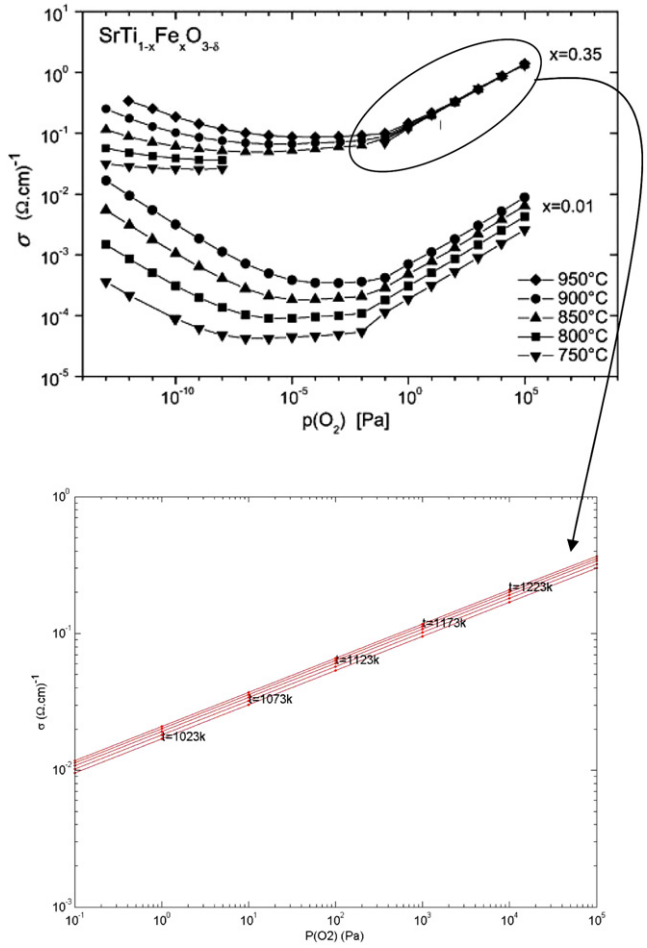


**Figure 6.** Electrical conductivity of $SrTi_{0.65}Fe_{0.35}O_{3-\delta}$ based sensors as a function of oxygen pressure for five different temperatures. (a) Measured results by Scott Litzelman [16] and (b) the calculated results (this work).

## 4. Comparison of the analytical with the reported results

Comparison of our calculated results with the reported experimental results for the sensing layers response of $CeO_2$ [12, 15] and $SrTi_{0.65}Fe_{0.35}O_{3-\delta}$ [16] will be accomplished in two separate sections. The $SrTi_{0.65}Fe_{0.35}O_{3-\delta}$ sensing layers act as p-type at high temperatures and $CeO_2$ layers as n-type oxide semiconductors.

### *4.1. The $SrTi_{0.65}Fe_{0.35}O_{3-\delta}$ based oxygen gas sensors*

Figure 5(a) shows the experimental and figure 5(b) the calculated temperature dependency of the $SrTi_{0.65}Fe_{0.35}O_{3-\delta}$ sensor results, respectively. Figure 5(a) gives three different measured results for sensors having three different sensing layers of grain sizes from 70 to 316 nm. The reported operating temperature range is 150 to 900 K and oxygen pressure is 1 Pa [16]. Our obtained equations do not take account of the grain size effect on the sensor response. Therefore, only a single plot in figure 5(b) is drawn using equation (12) considering the temperature range of 150–900 K and oxygen

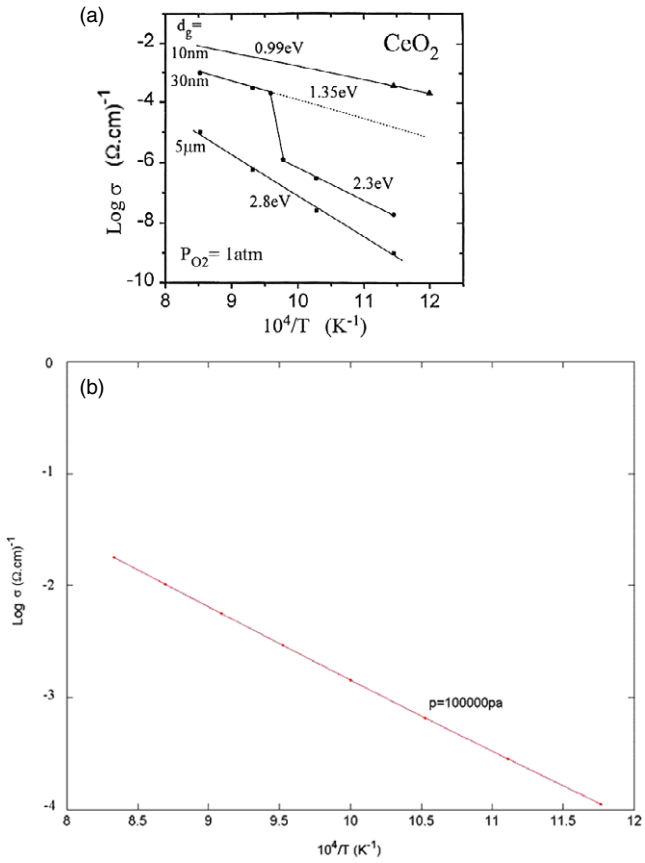


**Figure 7.** Conductivity versus temperature for $CeO_2$ based sensors. (a) The measured results by Igor Kosacki [17] and (b) the calculated results (this work).

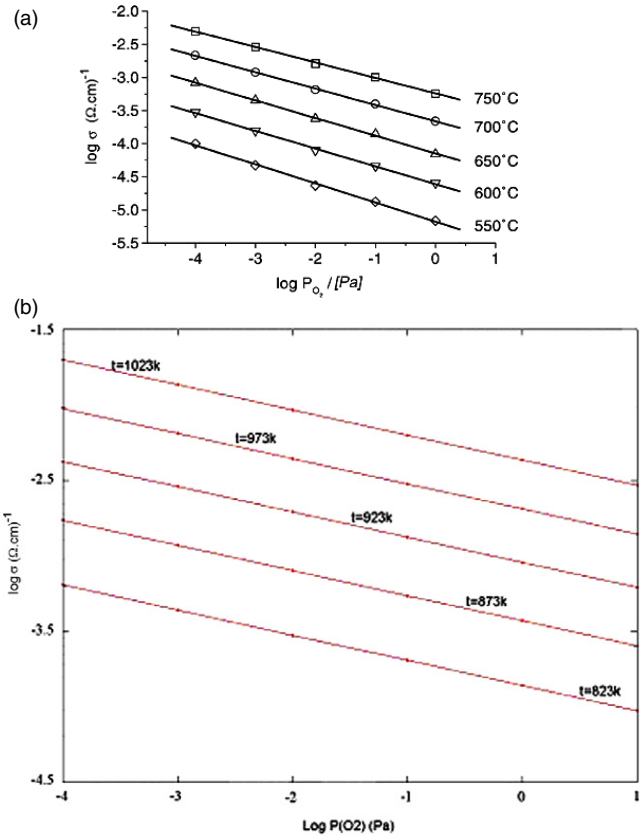


**Figure 8.** The response of ceria based sensors to oxygen pressure at different temperatures. (a) The calculated results (this work) and (b) the measured results by Piotr Jasinski [12].

pressure of 1 Pa. Comparing figures 5(a) and 5(b), we can conclude that our calculated results in figure 5(b) differ by less than 1% from the measured values of Scott Litzelman [16] as shown in figure 5(a) for the grain size of 158 nm.

Figure 6(a) shows the measured conductivity of $SrTi_{1-x}Fe0_xO_{3-\delta}$ based sensors versus oxygen pressure at five different operating temperatures. The $SrTi_{1-x}Fe_xO_{3-\delta}$ based sensors exhibit n-type semiconductor behavior at low oxygen pressures and p-type semiconductor behavior at high pressures. This behavior is indicative of a transition from n- to p-type conductivity at the corresponding pressure range, for $SrTi_{1-x}Fe_xO_{3-\delta}$ [16]. Figure 6(b) shows the calculated response of $SrTi_{0.65}Fe_{0.35}O_{3-\delta}$ based sensors at high oxygen pressure ($>10^{-1}$ Pa), i.e. in the p-type region. Comparing our calculated results of figure 6(b) with the right hand section of the measured results of figure 6(a) [16], having $x = 0.35$ (as indicated by an arrow), the mismatch is about 0.9%.

### *4.2. The n-type oxygen sensors based on $CeO_2$*

The measured operating temperature effect on the $CeO_2$ based oxygen sensor by Kosacki *et al*, is shown in figure 7(a) [15]. There are three plots showing the response of three sensors having sensing layers of grain sizes 10 nm, 30 nm, and 5 $\mu$m. The operating temperature range is 800–1250 K at an oxygen pressure of $10^5$ Pa [15]. In figure 7(b) our single calculated plot, using equation (11) and Matlab software, is shown. The calculation is carried out applying the same conditions as in the experiment, but without considering the grain size. Comparing our theoretical plots with the experimental ones figure 7(a) [15], we may conclude that our results match with the reported plot related to sensing layers of 10 nm grain size.

The measurement results reported by Piotr Jasinski [12] for the response of the resistive oxygen gas sensor based on ceria as a function of oxygen pressure, at different temperatures, are shown in figure 8(a). The calculated results employing equation (11) and Matlab software are shown in figure 8(b). The considered parameters in equation (11) are identical to the measurement conditions. Our calculated results of figure 8(a) are compared with the reported measured results of figure 8(b) [12], and the mismatch is about 0.8%. However, the analytically drawn plots are slightly shifted up compared to the reported plots.

## 5. Conclusion

The conductivity of the oxide semiconductor sensing layer of oxygen gas sensors is analytically studied. More precise equations, compared to those so far reported for the conductivity of the n-type and p-type oxide semiconductors, are derived. The analytical study includes most of the physical parameters affecting the sensing layer response to oxygen gas, such as mobility, Fermi energy, and energy gap.

However, the effect of the grain size of the sensing layer is not included in our work and should be studied. By applying the obtained equations and using Matlab software, we examined the responses of oxygen sensors based on $CeO_2$ and $SrTi_{0.65}Fe_{0.35}O_{3-\delta}$ as a function of temperature and oxygen gas pressures. The calculated results are compared with the reported measured results and in most cases there was a close agreement between them.

## References


[1] Wu Ch C and Luo Ch h 2004 Design and fabrication of micromachined sensors on energy consumption measurement for premature infants *PhD Thesis* National Cheng Kung University

[2] Vanhandel G J and Blumenthal R N 1974 The temperature and oxygen pressure dependence of the ionic transference number of nonstoichiometric $CeO_{2-x}$ *J. Electrochem. Soc.* **121** 1198–974

[3] Baban C, Toyoda Y and Ogita M 2005 Oxygen sensing at high temperatures using $Ga_2O_3$ films *Thin Solid Films* **484** 369–73

[4] Izu N, Shin W, Matsubara I and Murayama N 2004 Small temperature-dependent resistive oxygen gas sensors using $Ce_{0.9}Y_{0.1}O_2$ as a new temperature compensating material *Sensors Actuators* B **101** 381–6

[5] Izu N, Shin W, Matsubara I and Murayama N 2004 Kinetic behavior of resistive oxygen gas sensor using cerium oxide *Sensors Actuators* B **100** 411–6

[6] Izu N, Shin W, Matsubara I and Murayama N 2006 Evaluation of response characteristics of resistive oxygen sensors based on porous cerium oxide thick film using pressure modulation method *Sensors Actuators* B **113** 207–13

[7] Moos R, Enesklou W M, Schreiner H J and Hardtl K H 2000 Materials for temperature independent resistive oxygen gas sensors for combustion exhaust gas control *Sensors Actuators* B **67** 178–83

[8] Khodadadi A, Mohajerzadeh S S, Mortazavi Y and Miri A M 2003 Cerium oxide/$SnO_2$-based semiconductor gas sensors with improved sensitivity to CO *Sensors Actuators* B **80** 267–71

[9] Tabata S, Higaki K, Ohnishi H, Suzuki T, Kunihara K and Kobayashi M 2005 A micromachined gas sensor based on a catalytic thick film/SnO thin film bilayer and a thin film heater part 2: CO sensing *Sensors Actuators* B **109** 190–3

[10] Tsai P P, Chen I Ch and Ho Ch J 2001 Ultra low power carbon monoxide microsensor by micromachining techniques *Sensors Actuators* B **86** 380–7

[11] Izu N, Shin W, Matsubara I, Murayama N, Oh-hori N and Itou M 2005 Temperature independent resistive oxygen gas sensors using solid electrolyte zirconium as a new temperature compensating material, numerical analysis of response time for resistive oxygen gas sensors *Sensors Actuators* B **108** 216–22

[12] Jasinski P, Suzuki T and Anderson H U 2003 Nanocrystallite undoped ceria oxygen sensor *Sensors Actuators* B **95** 73–7

[13] Kittel Ch 1996 *Introduction to Solid State Physics* (New York: Wiley)

[14] Pankove J I 1971 *Optical Processes in Semiconductor* (New York: Dover) chapter 2 pp 22–33

[15] Kosacki I, Suzuki T, Petrovsky V and Anderson H U 2000 Electrical conductivity of nanocrystalline ceria and zirconium thin films *Solid State Ion.* **136/137** 1225–33

[16] Litzelman S J, Rothschild A and Tuller H L 2005 The electrical properties and stability of $SrTi_{0.65}Fe_{0.35}O_{3-\delta}$ thin films for automotive oxygen sensor application *Sensors Actuators* B **108** 231–7